# Pose2Gaze: Eye-body Coordination during Daily Activities for Gaze Prediction from Full-body Poses

Zhiming Hu, Jiahui Xu, Syn Schmitt, Andreas Bulling

*Abstract*—Human eye gaze plays a significant role in many virtual and augmented reality (VR/AR) applications, such as gaze-contingent rendering, gaze-based interaction, or eye-based activity recognition. However, prior works on gaze analysis and prediction have only explored eye-head coordination and were limited to human-object interactions. We first report a comprehensive analysis of eye-body coordination in various human-object and human-human interaction activities based on four public datasets collected in real-world (MoGaze), VR (ADT), as well as AR (GIMO and EgoBody) environments. We show that in human-object interactions, e.g. *pick* and *place*, eye gaze exhibits strong correlations with full-body motion while in human-human interactions, e.g. *chat* and *teach*, a person's gaze direction is correlated with the body orientation towards the interaction partner. Informed by these analyses we then present *Pose2Gaze* – a novel eye-body coordination model that uses a convolutional neural network and a spatio-temporal graph convolutional neural network to extract features from head direction and full-body poses, respectively, and then uses a convolutional neural network to predict eye gaze. We compare our method with state-of-the-art methods that predict eye gaze only from head movements and show that *Pose2Gaze* outperforms these baselines with an average improvement of 24.0% on MoGaze, 10.1% on ADT, 21.3% on GIMO, and 28.6% on EgoBody in mean angular error, respectively. We also show that our method significantly outperforms prior methods in the sample downstream task of eye-based activity recognition. These results underline the significant information content available in eye-body coordination during daily activities and open up a new direction for gaze prediction.

*Index Terms*—Eye-body coordination, human-object interaction, human-human interaction, gaze prediction, activity recognition, virtual reality, augmented reality

## I. INTRODUCTION

With the increasing use of virtual and augmented reality (VR/AR), understanding and predicting human behaviour in VR/AR environments has become a popular research topic and is a key requirement for intelligent human-aware VR/AR agents [1], [2]. Human eye movements are of particular interest given that they are key for important VR/AR applications, such as 1) gaze-contingent rendering that renders the gaze central region with high quality while decreasing the fidelity in peripheral region to increase rendering efficiency [3]; 2) gaze-based interaction that uses eye gaze to interact with 3D objects in virtual environments [4]; 3) virtual content optimisation that optimises the design of virtual content based on gaze distributions [5]; 4) gaze-guided redirected walking that redirects a

Zhiming Hu, Jiahui Xu, Syn Schmitt, and Andreas Bulling are with the University of Stuttgart, Germany. E-mail: {zhiming.hu@vis.uni-stuttgart.de, st170522@stud.uni-stuttgart.de, schmitt@simtech.uni-stuttgart.de, andreas.bulling@vis.uni-stuttgart.de}.

user's walking path based on their gaze directions [6]; or 5) eye-based activity recognition that recognises user activities from their eye movements [7].

Understanding and predicting human eye movements in VR/AR is challenging given the highly variable spatio-temporal dynamics of gaze allocation as well as various top-down influences, e.g. specific tasks that a user has to perform [1], [7] or social norms that a user ideally adheres to during interactions with humans [8]. Research on gaze behaviour analysis has revealed that eye movements are closely coordinated with head movements and, as such, that head orientation can be used as a proxy to eye gaze [1], [9]–[11]. Consequently, previous works have mainly focused on exploiting eye-head coordination for predicting eye movements [1], [10], [11] while neglecting coordination between eye and full-body movements. Furthermore, most existing works have studied human-object interactions [1], [7] and have neglected the more challenging but for VR/AR applications also more practically useful human-human interactions, in which a person's eye gaze is influenced by the body movements of the interaction partner.

To fill this gap, in this work we are the first to report comprehensive analyses of the correlations between gaze direction and full-body movements using four publicly available datasets collected in the real world (MoGaze [12]), in VR (ADT [13]) and AR (GIMO [14] and EgoBody [15]). These datasets contain human eye and full-body motion data recorded using a body tracking system and an eye tracker during various daily activities. Our analyses reveal that in human-object interactions, e.g. *pick*, *place*, *touch*, or *hold*, eye gaze exhibits strong correlations with full-body motion and eye movements precede body movements. In contrast, in human-human interactions, e.g. *chat*, *teach*, or *discuss*, a person's gaze is more closely correlated with the body orientation towards the interaction partner. Based on these findings we further present *Pose2Gaze* – the first method to predict eye movements from human full-body poses during human-object and human-human interactions. At the core of our method is a novel learning-based eye-body coordination model that based on a convolutional neural network (CNN) and a spatio-temporal graph convolutional neural network (GCN) to extract features from head directions and full-body poses, respectively. A convolutional neural network is also used to predict human eye gaze from these extracted features. We compare our method with state-of-the-art gaze prediction methods for three different prediction tasks, i.e. generating target eye gaze from past, present, and future body poses, respectively, and show that our method outperforms these baselines by a large margin in terms of mean angular error

on the MoGaze (24.0% improvement), ADT (10.1%), GIMO (21.3%), and EgoBody (28.6%) datasets. We also evaluate the effectiveness of our method for a sample downstream task, i.e eye-based activity recognition, and demonstrate that using our gaze prediction method results in significant improvements in recognition accuracy. [1]

The specific contributions of our work are four-fold:

- We provide comprehensive analyses of eye-body coordination in human-object and human-human interactions in the real world, VR, and AR, and show that eye gaze is strongly correlated with full-body motion in human-object interactions and is closely linked with the directions between two bodies in human-human interactions.
- We propose *Pose2Gaze* – a novel eye-body coordination model for gaze prediction that combines a CNN and a spatio-temporal GNN to extract features from head directions and full-body poses.
- We report extensive experiments on four public datasets for three different prediction tasks and demonstrate significant performance improvements over several state-of-the-art methods.
- We demonstrate our method's effectiveness in the sample downstream task of eye-based activity recognition.

## II. RELATED WORK

Our work is related to previous research on 1) human movement prediction, 2) eye-body coordination, as well as 3) eye gaze prediction.

### A. Human Movement Prediction

Human movement prediction is an important research topic in the areas of virtual reality and augmented reality. Some researchers focused on predicting human body movements from speech signals. For example, Hasegawa et al. used recurrent neural networks (RNNs) to generate natural human full-body poses from perceptual features extracted from the input speech audio [16] while Kucherenko et al. employed autoencoder neural networks to learn latent representations for human poses and speech signals and then learned the mappings between the two representations to predict human body motions [17]. Other researchers used the text transcripts of speech to generate human poses. Specifically, Yoon et al. proposed to use a RNN-based encoder to extract features from speech text and a RNN-based decoder to generate human poses [18] while Bhattacharya et al. employed an end-to-end Transformer network to predict human movements from the text transcripts of speech [19]. In addition, there also exist some works that generated human dance motions from input music and achieved good performances [20], [21]. While previous works typically focused on generating human body movements, they neglected the prediction of human eye gaze, which is significant for human-human [22], [23] and human-computer interactions [4], [24], [25]. In this work, we focus on predicting human eye movements directly from human full-body poses to fill this gap.

---

[1]The full source code and trained models will be released upon acceptance.

### B. Eye-body Coordination

The coordination of human eye and body movements is an important research topic in the areas of cognitive science and human-centred computing. Many researchers focused on the coordinated movements between the eyes and the head [10], [26], [27]. Specifically, Stahl analysed the process of gaze shifts and found its amplitude to be proportional to that of head movements [26]. Fang et al. further examined eye-head coordination during visual search in a large visual field and found that eye-head coordination plays an important role in visual cognitive processing [27]. Hu et al. revealed that human eye movements are strongly correlated with head movements in both free-viewing [10], [11] and task-oriented settings [1], [7] in immersive virtual environments while Kothari et al. identified the coordination of eye and head movements in real-world daily activities [28]. Recently, some researchers went beyond eye-head coordination to investigate the correlations between eye movements and the movements of different body parts. For example, Sidenmark et al. focused on the gaze shift process in immersive virtual reality and discovered general eye, head, and torso coordination patterns [29]. Batmaz et al. developed a VR training system based on the coordination of eye and hand movements and compared user performance in three different virtual environments [30]. Emery et al. collected a large-scale dataset that contains human eye, hand, and head movements in a virtual environment and identified the coordination of eye, hand, and head motions [31]. Randhavane et al. investigated the effectiveness of eye-gait coordination on expressing emotions and further employed gaze and gait features to generate various emotions for virtual agents [32]. However, prior works typically focused on the correlations between eye gaze and a particular body part, e.g. head, hand, or torso. In contrast, we are the first to study the coordinations of eye and full-body movements simultaneously, which paves the way for predicting eye gaze from full-body poses.

### C. Eye Gaze Prediction

Eye gaze prediction is a popular research topic in the areas of computer vision and human-centred computing. Typical gaze prediction methods can be classified into bottom-up and top-down approaches. Bottom-up methods predict eye gaze from the low-level image features of the scene content such as intensity, colour, and orientation [33], [34]. For example, Itti et al. used multiscale colour, intensity, and orientation features extracted from the image to predict saliency map (density map of eye gaze distribution) [33] while Cheng et al. employed the global contrast features of the image to generate saliency map [34]. Top-down approaches take high-level features of the scene such as specific tasks and context information into consideration to predict eye gaze [35], [36]. For example, Borji et al. employed players' input such as 2D mouse positions and joystick buttons to predict their eye gaze [35] while Koulieris et al. used game state variables to predict users' eye gaze positions in video games [36]. In addition to the typical bottom-up and top-down approaches, recently some researchers took the eye-head coordination into consideration and attempted to predict eye gaze from human head movements [9], [10].

Specifically, Nakashima et al. proposed to use head directions as prior knowledge to improve the accuracy of bottom-up saliency prediction methods through simple multiplication of the predicted saliency map by a Gaussian head direction bias [37]. Sitzmann et al. employed users' head orientations to predict saliency maps for 360-degree images and achieved an accuracy that is on par with the performance of bottom-up saliency predictors [9]. Hu et al. proposed to use users' head rotation velocities to predict users' eye gaze positions in immersive virtual environments and achieved good performances [1], [38]. However, existing works have only explored the effectiveness of head movements on the task of eye gaze prediction and were limited to human-object interactions. In stark contrast, in this work we investigate the effectiveness of full-body movements on predicting human eye gaze in both human-object and human-human interaction activities.

## III. ANALYSIS OF EYE-BODY COORDINATION

### A. Gaze and Pose Data

We studied the eye-body coordination from two perspectives, i.e. the correlation between gaze direction and body orientations and the correlation between gaze direction and body motions (translational movements of the body). We conducted a comprehensive analysis based on four public datasets that contain various human-object and human-human interaction activities collected from the real world (MoGaze [12]), VR environments (ADT [13]), as well as AR scenarios (GIMO [14] and EgoBody [15]).

*a) MoGaze:* The MoGaze dataset contains 180 minutes of full-body motion capture data collected from seven participants performing everyday *pick* and *place* activities in an indoor environment. One participant's eye gaze data is not recorded. Therefore, we only used the data from six people to analyse eye-body coordination.

*b) ADT:* The ADT dataset collects human eye gaze and/or full-body pose data performing various indoor activities in two virtual environments (an apartment and an office environment). To analyse eye-body coordination, we used the 34 sequences that contain both eye gaze and full-body pose data. Each sequence lasts for around 2 minutes and the activities include *decoration*, *meal*, and *work*.

*c) GIMO:* The GIMO dataset records eye gaze and full-body poses from 11 people performing various daily activities in various indoor scenes. The whole dataset contains 215 sequences and each sequence lasts for around 10 seconds. The activities can be classified into three categories, i.e. *change the state of objects* (*open*, *push*, *transfer*, *throw*, *pick up*, *lift*, *connect*, *screw*, *grab*, *swap objects*), *interact with objects* (*touch*, *hold*, *step on*, *reach to objects*), and *rest* (*sit* or *lay on objects*). The original dataset does not provide activity labels for each sequence. To gain a comprehensive analysis, we manually labelled each sequence as one of the three categories.

*d) EgoBody:* The EgoBody dataset collects eye gaze and full-body pose data from 36 people performing diverse human-human interaction activities (between two humans) in 15 indoor scenes. The whole dataset contains 125 sequences and each sequence lasts for around 2 minutes. The activities include *catch*, *chat*, *dance*, *discuss*, *learn*, *perform*, and *teach*.

TABLE I
THE COSINE SIMILARITIES BETWEEN EYE GAZE DIRECTION AND THE DIRECTIONS OF DIFFERENT BODY JOINTS IN THE MoGAZE, GIMO, AND EGOBODY DATASETS. GAZE DIRECTION IS STRONGLY CORRELATED WITH BODY ORIENTATIONS, ESPECIALLY WITH HEAD DIRECTION.

|  |  | base | pelvis | torso | neck | head |
|---|---|---|---|---|---|---|
| MoGaze | pick | 0.64 | 0.60 | 0.66 | 0.84 | 0.92 |
|  | place | 0.62 | 0.58 | 0.63 | 0.84 | 0.92 |
| GIMO | change | 0.76 | 0.86 | 0.86 | 0.90 | 0.93 |
|  | interact | 0.72 | 0.82 | 0.83 | 0.87 | 0.93 |
|  | rest | 0.67 | 0.82 | 0.83 | 0.87 | 0.92 |
| EgoBody | catch | 0.90 | 0.94 | 0.94 | 0.96 | 0.97 |
|  | chat | 0.81 | 0.85 | 0.87 | 0.90 | 0.94 |
|  | dance | 0.82 | 0.86 | 0.87 | 0.93 | 0.97 |
|  | discuss | 0.88 | 0.88 | 0.91 | 0.93 | 0.94 |
|  | learn | 0.70 | 0.75 | 0.77 | 0.84 | 0.89 |
|  | perform | 0.90 | 0.92 | 0.92 | 0.95 | 0.97 |
|  | teach | 0.84 | 0.84 | 0.86 | 0.89 | 0.93 |

### B. Correlation between Eye Gaze and Body Orientations

Prior works have mainly focused on the correlation between eye gaze and head directions [10], [11]. To gain a comprehensive understanding of eye-body coordination, we simultaneously analysed the correlation between eye gaze and the orientations of different body joints, e.g. *neck* and *torso*. The ADT dataset does not provide the orientations of the body joints and therefore we only performed analysis on the MoGaze, GIMO, and EgoBody datasets. Specifically, we employed the forward directions of the body joints to represent body orientations and used the cosine similarity to analyse the correlation between eye gaze and body orientations. Cosine similarity measures the similarity between two non-zero vectors by calculating the cosine of the angle between the vectors and produces a value in the range from $-1$ to $+1$, where $-1$ indicates perfect negative correlation, $0$ denotes no correlation, and $+1$ represents perfect positive correlation. Table I summarises the cosine similarities between eye gaze direction and the directions of different body joints in the MoGaze, GIMO, and EgoBody datasets. We can see that most of the cosine similarities are larger than $0.6$, demonstrating that eye gaze has very high correlations with body orientations in various daily activities. In particular, we find that in all the activities eye gaze consistently exhibits highest correlation with head direction ($> 0.9$ in most cases), validating that head direction correlates better with eye gaze than other body orientations.

To investigate whether there exist time delays between eye gaze and head orientations, we desynchronised the gaze and head signals by adding different time intervals between them (time interval $> 0$ means head data is moved forward in time while time interval $< 0$ means gaze data is moved forward) and further calculated their cosine similarities. We can see from Figure 1 that head direction achieves its highest correlation with eye gaze at the time interval of between $-100$ and $200\ ms$, indicating that there exists little or no time delay between head and eye movements. These results further validate that head direction is a suitable proxy for eye gaze in
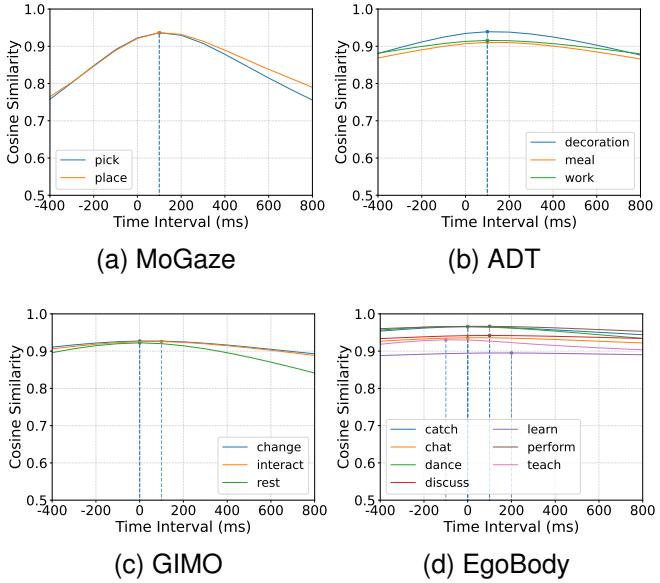
Fig. 1. The cosine similarities between head and gaze directions at different time intervals in the (a) MoGaze (b) ADT (c) GIMO and (d) EgoBody datasets. The highest correlations occur at between $-100$ and $200\ ms$, suggesting that there is little or no time delay between head and eye movements.
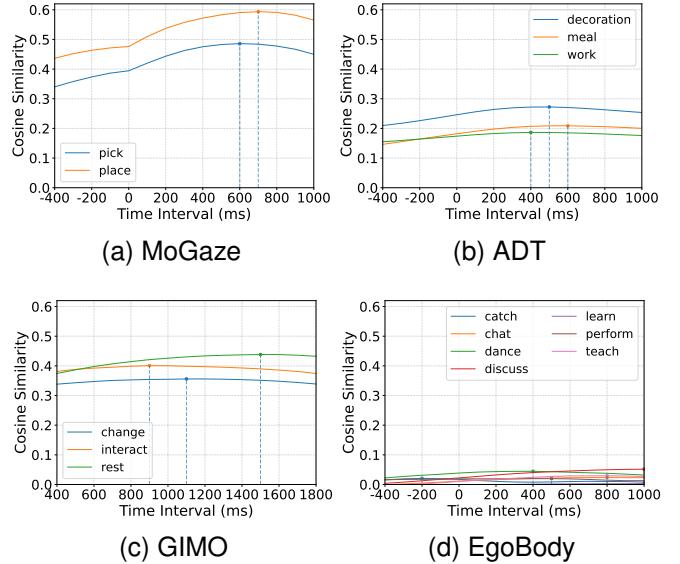


Fig. 2. The cosine similarities between eye gaze and body motions at different time intervals in the (a) MoGaze (b) ADT (c) GIMO and (d) EgoBody datasets. The highest correlations occur at between 400 and 1500 $ms$, indicating that eye movements precede body motions.

everyday activities.

### C. Correlations between Eye Gaze and Body Motions

To analyse the correlations between human eye gaze and human full-body motion, we calculated the velocities of different body joints using the difference in position between two consecutive frames and then normalised these velocities to 3D unit vectors to represent the directions of body motions. We further calculated the cosine similarities between eye gaze and the directions of body motions to measure their correlations. Table II shows the cosine similarities between eye gaze and full-body motions in the MoGaze, ADT, GIMO, and EgoBody datasets. We find that in the human-object interaction activities, e.g. *pick*, *place*, *decoration*, *change*, and *interact*, eye gaze exhibits strong correlations with full-body motions ($> 0.3$ in most cases). In the *meal* and *work* activities, the eye-body correlations are relatively smaller, probably because the body motions are less frequent in such activities and are thus less correlated with eye gaze. In the human-human interaction activities, e.g. *chat*, *discuss*, and *learn*, we find that eye gaze has little or no correlation with body motions ($\leq$ 0.05 in most cases). This is probably because a person's eye and body motion are strongly influenced by the interaction partner in human-human interactions, thus degrading the eye-body correlations.

To investigate any potential time delays between body motions and eye movements, we added different time intervals between body motions and gaze directions (time interval $> 0$ means body motion data is moved forward in time while time interval $< 0$ means gaze data is moved forward) and further calculated their correlations. Specifically, we first calculated the cosine similarities between eye gaze and the motions of

different body joints and then averaged the cosine similarities across all the body joints. We can see from Figure 2 that in human-object interaction activities the highest correlations occur at between 400 and 1500 $ms$, suggesting that there exists a noticeable time delay between body motions and eye movements, i.e. eye movements precede body motions. In the human-human interaction activities, we find that the eye-body correlations are consistently small ($< 0.1$ in all the cases) at different time intervals, validating that there is little or no correlation between eye gaze and body motion in human-human interactions.

### D. Eye-body Coordination in Human-human Interactions

To analyse the influence of the interaction partner on a person's eye gaze during human-human interactions, we calculated the directions pointing from a person's body joints to the body joints of the interaction partner (see Figure 3a). To this end we used the difference in position between the person and the interaction partner and normalised these directions to 3D unit vectors. We further calculated the cosine similarities between eye gaze and the directions between two bodies to measure their correlation. We can see in Table III that eye gaze is highly correlated with the directions between both bodies ($> 0.9$ in most cases), suggesting that a person's eye gaze is significantly influenced by the interaction partner in human-human interactions. Figure 3b further shows the cosine similarities between eye gaze and the directions between two bodies at different time intervals. We can see that the highest correlations either occur at 0 $ms$ or are very close to the correlation values at 0 $ms$, meaning that there is little or no time delay between body motions and eye movements in human-human interactions.

TABLE II

THE COSINE SIMILARITIES BETWEEN EYE GAZE AND THE MOTIONS OF DIFFERENT BODY JOINTS IN THE MOGAZE, ADT, GIMO, AND EGOBODY DATASETS. EYE GAZE HAS STRONG CORRELATIONS WITH BODY MOTIONS IN HUMAN-OBJECT INTERACTION ACTIVITIES WHILE HAVING LITTLE OR NO CORRELATION IN HUMAN-HUMAN INTERACTION ACTIVITIES. l_col: left collar, r_col: right collar, l_sho: left shoulder, r_sho: right shoulder, l_elb: left elbow, r_elb: right elbow, l_wri: left wrist, r_wri: right wrist, l_hip: left hip, r_hip: right hip, l_kne: left knee, r_kne: right knee, l_ank: left ankle, r_ank: right ankle, l_toe: left toe, r_toe: right toe.

| | | base | pelvis | torso | neck | head | l_col | r_col | l_sho | r_sho | l_elb | r_elb | l_wri | r_wri | l_hip | r_hip | l_kne | r_kne | l_ank | r_ank | l_toe | r_toe | Average |
|---|---|---|---|---|---|---|---|---|---|---|---|---|---|---|---|---|---|---|---|---|---|---|---|
| MoGaze | pick | 0.40 | 0.40 | 0.41 | 0.42 | 0.46 | 0.42 | 0.42 | 0.38 | 0.41 | 0.35 | 0.40 | 0.34 | 0.46 | 0.40 | 0.40 | 0.42 | 0.42 | 0.31 | 0.32 | 0.37 | 0.37 | 0.39 |
| | place | 0.48 | 0.49 | 0.49 | 0.50 | 0.54 | 0.50 | 0.50 | 0.47 | 0.48 | 0.44 | 0.47 | 0.43 | 0.58 | 0.49 | 0.48 | 0.50 | 0.50 | 0.39 | 0.39 | 0.45 | 0.45 | 0.48 |
| ADT | decoration | 0.28 | 0.28 | 0.26 | 0.26 | 0.27 | 0.26 | 0.26 | 0.26 | 0.24 | 0.27 | 0.23 | 0.31 | 0.25 | 0.28 | 0.28 | 0.28 | 0.26 | 0.15 | 0.12 | 0.20 | 0.14 | 0.25 |
| | meal | 0.20 | 0.20 | 0.20 | 0.20 | 0.20 | 0.20 | 0.20 | 0.20 | 0.19 | 0.19 | 0.20 | 0.22 | 0.22 | 0.20 | 0.20 | 0.20 | 0.20 | 0.09 | 0.08 | 0.13 | 0.10 | 0.18 |
| | work | 0.18 | 0.19 | 0.19 | 0.20 | 0.22 | 0.20 | 0.20 | 0.20 | 0.18 | 0.19 | 0.17 | 0.20 | 0.18 | 0.18 | 0.18 | 0.19 | 0.18 | 0.10 | 0.09 | 0.14 | 0.10 | 0.17 |
| GIMO | change | 0.34 | 0.34 | 0.35 | 0.35 | 0.34 | 0.35 | 0.35 | 0.34 | 0.34 | 0.33 | 0.33 | 0.29 | 0.32 | 0.34 | 0.34 | 0.31 | 0.31 | 0.19 | 0.17 | 0.15 | 0.10 | 0.30 |
| | interact | 0.38 | 0.38 | 0.37 | 0.37 | 0.36 | 0.37 | 0.37 | 0.36 | 0.36 | 0.35 | 0.36 | 0.32 | 0.36 | 0.38 | 0.38 | 0.35 | 0.34 | 0.21 | 0.21 | 0.18 | 0.15 | 0.33 |
| | rest | 0.36 | 0.35 | 0.35 | 0.34 | 0.34 | 0.35 | 0.35 | 0.34 | 0.34 | 0.32 | 0.32 | 0.30 | 0.32 | 0.36 | 0.37 | 0.33 | 0.33 | 0.20 | 0.18 | 0.17 | 0.14 | 0.31 |
| EgoBody | catch | 0.03 | 0.02 | 0.02 | 0.01 | 0.02 | 0.02 | 0.01 | 0.03 | 0.00 | 0.03 | -0.02 | 0.04 | 0.00 | 0.03 | 0.02 | 0.02 | 0.02 | 0.02 | 0.00 | 0.02 | 0.01 | 0.02 |
| | chat | 0.01 | 0.01 | 0.01 | 0.02 | 0.02 | 0.01 | 0.01 | 0.02 | 0.02 | 0.01 | 0.01 | 0.01 | 0.02 | 0.01 | 0.01 | 0.00 | 0.01 | 0.01 | 0.01 | 0.01 | 0.01 | 0.01 |
| | dance | 0.05 | 0.05 | 0.05 | 0.04 | 0.04 | 0.04 | 0.05 | 0.04 | 0.04 | 0.03 | 0.04 | 0.03 | 0.03 | 0.05 | 0.05 | 0.05 | 0.04 | 0.02 | 0.01 | 0.02 | 0.02 | 0.04 |
| | discuss | 0.02 | 0.02 | 0.03 | 0.03 | 0.04 | 0.03 | 0.03 | 0.04 | 0.03 | 0.02 | 0.03 | 0.03 | 0.03 | 0.01 | 0.01 | 0.00 | 0.02 | 0.00 | 0.00 | 0.01 | 0.01 | 0.02 |
| | learn | 0.00 | -0.01 | -0.01 | -0.01 | -0.01 | -0.01 | 0.00 | -0.01 | 0.00 | -0.01 | -0.01 | -0.01 | 0.00 | 0.00 | -0.01 | -0.01 | 0.00 | 0.01 | 0.01 | 0.01 | 0.00 | 0.00 |
| | perform | 0.04 | 0.04 | 0.02 | 0.02 | 0.01 | 0.01 | 0.03 | -0.01 | 0.01 | -0.03 | 0.01 | 0.01 | 0.02 | 0.04 | 0.05 | 0.03 | 0.01 | 0.01 | 0.03 | 0.02 | 0.03 | 0.02 |
| | teach | 0.00 | 0.00 | 0.01 | 0.01 | 0.02 | 0.01 | 0.01 | 0.00 | 0.02 | 0.00 | 0.02 | 0.01 | 0.02 | 0.00 | 0.01 | 0.01 | 0.02 | 0.02 | 0.02 | 0.02 | 0.02 | 0.01 |

TABLE III

THE COSINE SIMILARITIES BETWEEN EYE GAZE AND THE DIRECTIONS POINTING FROM A PERSON'S BODY TO THE INTERACTION PARTNER IN HUMAN-HUMAN INTERACTION ACTIVITIES. EYE GAZE IS HIGHLY CORRELATED WITH THE DIRECTIONS BETWEEN TWO BODIES. l_col: left collar, r_col: right collar, l_sho: left shoulder, r_sho: right shoulder, l_elb: left elbow, r_elb: right elbow, l_wri: left wrist, r_wri: right wrist, l_hip: left hip, r_hip: right hip, l_kne: left knee, r_kne: right knee, l_ank: left ankle, r_ank: right ankle, l_toe: left toe, r_toe: right toe.

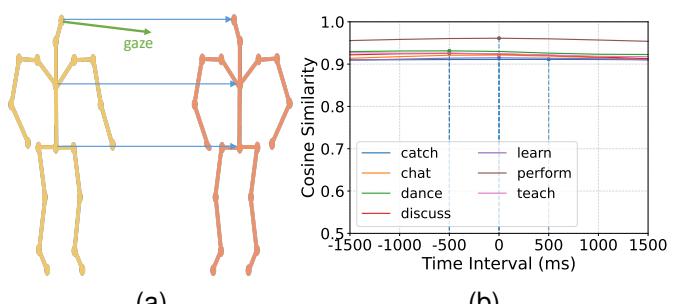| | | base | pelvis | torso | neck | head | l_col | r_col | l_sho | r_sho | l_elb | r_elb | l_wri | r_wri | l_hip | r_hip | l_kne | r_kne | l_ank | r_ank | l_toe | r_toe | Average |
|---|---|---|---|---|---|---|---|---|---|---|---|---|---|---|---|---|---|---|---|---|---|---|---|
| | catch | 0.92 | 0.92 | 0.92 | 0.92 | 0.91 | 0.92 | 0.92 | 0.91 | 0.91 | 0.90 | 0.90 | 0.89 | 0.89 | 0.92 | 0.92 | 0.91 | 0.91 | 0.92 | 0.91 | 0.91 | 0.90 | 0.91 |
| | chat | 0.94 | 0.94 | 0.94 | 0.94 | 0.94 | 0.94 | 0.94 | 0.92 | 0.93 | 0.91 | 0.91 | 0.89 | 0.89 | 0.93 | 0.93 | 0.91 | 0.92 | 0.91 | 0.91 | 0.89 | 0.89 | 0.92 |
| | dance | 0.95 | 0.95 | 0.95 | 0.95 | 0.95 | 0.95 | 0.95 | 0.94 | 0.94 | 0.91 | 0.92 | 0.87 | 0.90 | 0.94 | 0.95 | 0.92 | 0.93 | 0.91 | 0.93 | 0.89 | 0.92 | 0.93 |
| EgoBody | discuss | 0.93 | 0.93 | 0.93 | 0.93 | 0.94 | 0.93 | 0.93 | 0.93 | 0.92 | 0.92 | 0.90 | 0.91 | 0.88 | 0.93 | 0.93 | 0.92 | 0.92 | 0.92 | 0.92 | 0.91 | 0.91 | 0.92 |
| | learn | 0.93 | 0.92 | 0.92 | 0.92 | 0.92 | 0.92 | 0.92 | 0.92 | 0.92 | 0.90 | 0.91 | 0.87 | 0.91 | 0.92 | 0.92 | 0.91 | 0.92 | 0.91 | 0.92 | 0.89 | 0.91 | 0.91 |
| | perform | 0.97 | 0.97 | 0.97 | 0.97 | 0.97 | 0.97 | 0.97 | 0.97 | 0.96 | 0.96 | 0.95 | 0.95 | 0.94 | 0.97 | 0.97 | 0.96 | 0.95 | 0.96 | 0.95 | 0.96 | 0.94 | 0.96 |
| | teach | 0.93 | 0.93 | 0.93 | 0.93 | 0.93 | 0.93 | 0.93 | 0.92 | 0.93 | 0.91 | 0.92 | 0.90 | 0.91 | 0.93 | 0.93 | 0.92 | 0.93 | 0.92 | 0.92 | 0.91 | 0.92 | 0.92 |



Fig. 3. (a) Eye gaze and the directions pointing from a person's body to the body of the interaction partner and (b) the cosine similarities between eye gaze and the directions between two bodies at different time intervals. The highest correlations either occur at 0 $ms$ or are very close to the correlation values at 0 $ms$, suggesting that there is little or no time delay between body motions and eye gaze.

*E. Summary*

Through comprehensive analyses we found that in various daily activities, eye gaze is closely correlated with body orientations, especially with head direction, and there is little or no time delay between head and eye movements. In human-object interactions, we find that eye gaze is strongly correlated with human full-body motions and eye movements precede body motions. In human-human interactions, we reveal that eye gaze has little or no correlation with body motions while having high correlations with the directions pointing from a person to the interaction partner and that there is little or no time delay between body motions and eye movements. These results suggest that head directions and full-body poses contain rich information about eye gaze and thus can be used to predict eye movements.

## IV. POSE2GAZE: EYE-BODY COORDINATION MODEL

### A. Model Design

*a) Design of Pose2Gaze:* The analyses in section III revealed that eye gaze is closely correlated with body orientations as well as full-body motions. Based on these insights, we propose an eye-body coordination model for gaze prediction that consists of three main components: a body orientation feature extraction module that extracts orientation features, a body motion feature extraction module that extracts motion features, and an eye gaze generation module that generates gaze directions from the extracted body orientation and motion features (see Figure 4 for an overview of our method). In the body orientation feature extraction module, we use head direction as input since it has higher correlation with eye gaze than other body orientations (see Table I). In the body motion feature extraction module, we use human full-body poses as
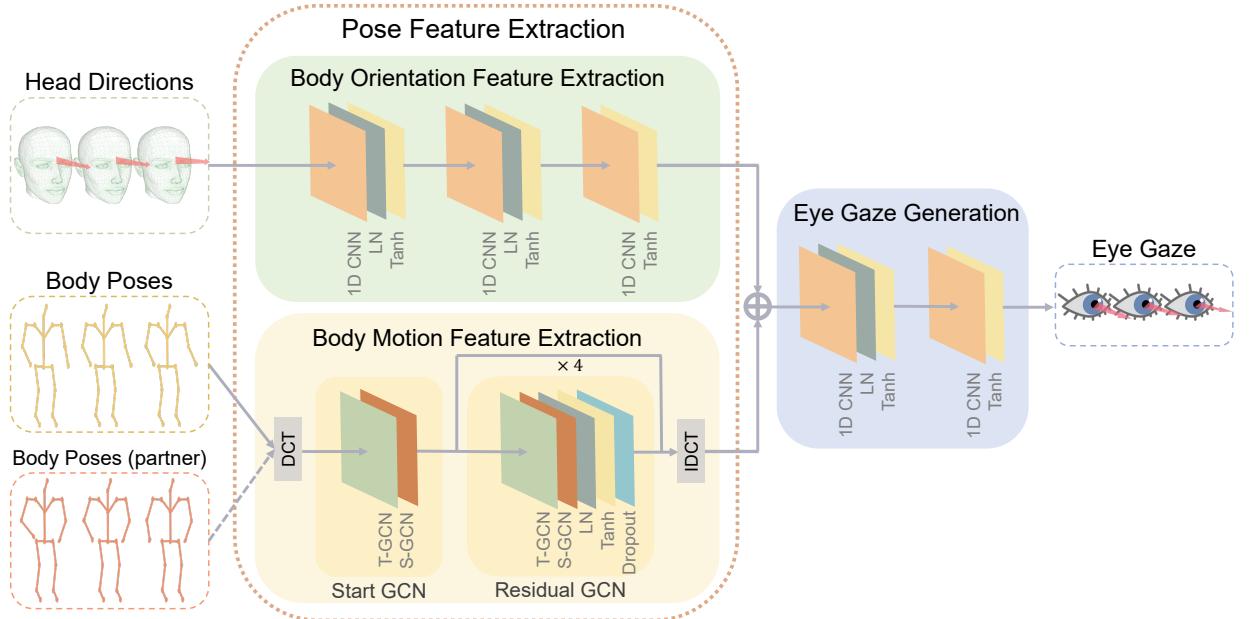
Fig. 4. Architecture of the proposed *Pose2Gaze* model. *Pose2Gaze* first uses a 1D convolutional neural network to extract body orientation features from head directions, then applies a spatio-temporal graph convolutional neural network to extract the body motion features from human full-body poses, and finally employs a 1D convolutional neural network to generate human eye gaze from the extracted body orientation and motion features.

input in human-object interaction activities since eye gaze is strongly correlated with full-body motions in this situation (see Table II) and employ the full-body poses of both the person and their interaction partner as input in human-human interactions considering that eye gaze has high correlations with the directions pointing from a person to the interaction partner in this setting (see Table III).

*b) Problem Formulation:* We define pose-based eye gaze prediction as the task of generating a sequence of eye gaze directions $G_{t+1:t+T} = \{g_{t+1}, g_{t+2}, ..., g_{t+T}\} \in R^{3 \times T}$, where $g$ is a 3D unit vector and $T$ is the length of the target eye gaze sequence, from human body orientations and motions. We use a sequence of head directions $H_{t+1+\Delta t_h:t+T+\Delta t_h} = \{h_{t+1+\Delta t_h}, h_{t+2+\Delta t_h}, ..., h_{t+T+\Delta t_h}\} \in R^{3 \times T}$ to represent body orientations, where $h$ is a 3D unit vector and $\Delta t_h$ is the time interval between the input head directions and target eye gaze. We employ a sequence of the 3D positions of all human joints $P_{t+1+\Delta t_p:t+T+\Delta t_p} = \{p_{t+1+\Delta t_p}, p_{t+2+\Delta t_p}, ..., p_{t+T+\Delta t_p}\} \in R^{3 \times N \times T}$ to represent body motions, where $N$ is the number of human joints and $\Delta t_p$ is the time interval between the input body poses and target eye gaze.

### B. Body Orientation Feature Extraction

In light of the good performance of 1D convolutional neural network for processing head movement data [1], [7], [11], we employed three 1D CNN layers to extract body orientation features from the sequence of head directions. Specifically, we used two 1D CNN layers, each with 32 channels and a kernel size of three, to process the head direction sequence $H \in R^{3 \times T}$. Each CNN layer was followed by a layer normalisation (LN) and a Tanh activation function. After the two CNN layers, we used a 1D CNN layer with 32 channels

and a kernel size of three, and a Tanh activation function to obtain the body orientation features $f_{ori} \in R^{32 \times T}$.

### C. Body Motion Feature Extraction

Given the effectiveness of discrete cosine transform (DCT) for extracting temporal features from human pose data [39], [40], we first employed DCT to encode human pose $P \in R^{3 \times N \times T}$ in the temporal domain using DCT matrix $M_{dct} \in R^{T \times T}$:

$$P_{dct} = PM_{dct}, \tag{1}$$

where $P_{dct} \in R^{3 \times N \times T}$ is the human pose after DCT transform. Considering that graph convolutional network outperforms other architectures like Transformer or RNN for processing human pose data [39], we propose two GCN blocks, i.e. a start GCN block and a residual GCN block, to extract motion features from the transformed pose data.

*a) Start GCN Block:* The start GCN block first applies a temporal GCN (T-GCN) to extract the temporal features from the transformed pose data $P_{dct}$. The temporal GCN views the pose data as a fully-connected graph that contains $T$ nodes corresponding to pose data at $T$ time steps. It learns the weighted adjacency matrix $A^T \in R^{T \times T}$ of the fully-connected temporal graph and performs temporal convolution using

$$f_{temp} = P_{dct}A^T, \tag{2}$$

where $f_{temp} \in R^{3 \times N \times T}$ is the extracted temporal features. $f_{temp}$ was then permuted to $f_{temp} \in R^{T \times N \times 3}$. A weight matrix $W^{start} \in R^{3 \times 16}$ was applied to convert the input node features (3 dimensions) to latent features (16 dimensions):

$$f_{lat} = f_{temp}W^{start}, \tag{3}$$

where $f_{lat} \in R^{T \times N \times 16}$ is the latent features. After the weight matrix, a spatial GCN (S-GCN) was applied to extract the spatial features. The spatial GCN views the latent features $f_{lat}$ as a fully-connected graph that contains $N$ nodes corresponding to $N$ human joints. S-GCN learns the weighted adjacency matrix $A^S \in R^{N \times N}$ of the fully-connected spatial graph and performs spatial convolution using

$$f_{spa} = A^S f_{lat}, \tag{4}$$

where $f_{spa} \in R^{T \times N \times 16}$ is the extracted spatial features. $f_{spa}$ was further permuted to $f_{spa} \in R^{16 \times N \times T}$. The output of the spatial GCN is copied along the temporal dimension ($R^{16 \times N \times T} \to R^{16 \times N \times 2T}$) to enhance the features [39] and is then used as input to the residual GCN block.

*b) Residual GCN Block:* The residual GCN block contains 4 GCN components with each component consisting of a temporal GCN that learns the temporal adjacency matrix $A_i^T \in R^{2T \times 2T}$, a weight matrix $W_i^{res} \in R^{16 \times 16}$ that extracts the latent features, a spatial GCN that learns the spatial adjacency matrix $A_i^S \in R^{N \times N}$, a layer normalisation, a Tanh activation function, and a dropout layer with dropout rate $0.3$ to avoid overfitting. We added a residual connection for each GCN component to improve the network flow. We further cut the output of the residual GCN block in half in the temporal dimension to reduce the feature dimensions.

The output of the residual GCN block was converted back to the original representation space using an inverse discrete cosine transform (IDCT) [39]. A Tanh activation function was applied after the IDCT to obtain the spatio-temporal human body motion features $f_{mot} \in R^{16 \times N \times T}$.

### D. Eye Gaze Generation

To generate eye gaze from the extracted body orientation and motion features, we first aggregated the body motion features $f_{mot}$ along the spatial dimension, i.e. concatenated the features of different body joints into a single motion feature ($R^{16 \times N \times T} \to R^{16N \times T}$). We then fused the extracted orientation and motion features by concatenating them along the spatial dimension and obtained $f \in R^{(16N+32) \times T}$. We finally used a 1D convolutional neural network to generate eye gaze from the fused features. Specifically, we used two CNN layers, each with a kernel size of three, to process the fused features. The first CNN layer has $64$ channels and is followed by a layer normalisation and a Tanh activation function while the second CNN layer uses three channels and a Tanh activation function to generate the eye gaze. The generated eye gaze directions were finally normalised to unit vectors: $\hat{G}_{t+1:t+T} = \{\hat{g}_{t+1}, \hat{g}_{t+2}, ..., \hat{g}_{t+T}\} \in R^{3 \times T}$.

### E. Loss Function

To train our model, we used the mean angular error between the generated eye gaze directions $\hat{G}_{t+1:t+T}$ and the ground truth gaze directions $G_{t+1:t+T}$ as our loss function:

$$\ell = \frac{1}{T} \sum_{j=t+1}^{t+T} \arccos(\hat{g}_j \cdot g_j). \tag{5}$$

## V. EXPERIMENTS AND RESULTS

We conducted extensive experiments to evaluate the performance of our gaze prediction model. Specifically, we compared our model with state-of-the-art gaze prediction methods that estimate eye gaze from head movements on the MoGaze, ADT, GIMO, and EgoBody datasets. We tested these methods under three different generation settings, i.e. generating target eye gaze from past, present, and future body poses, respectively. We also performed an ablation study to evaluate the effectiveness of each component used in our model.

### A. Experimental Settings

*a) Datasets:* We evaluated our method on the MoGaze, ADT, GIMO, and EgoBody datasets (see subsection III-A for the details of these datasets). On the MoGaze dataset, we performed a leave-one-person-out cross-validation to evaluate our model's generalisation capability for different users: We trained on the data from five people and tested on the remaining one, repeated this procedure six times by testing for a different target person, and calculated the average performance across all six iterations. On the ADT dataset, we randomly selected $24$ sequences for training and used the remaining $10$ sequences for testing. On the GIMO dataset, we used the default training and test sets provided by the authors [14], i.e. we used data from $12$ scenes for training ($178$ sequences) and data from $14$ scenes ($12$ known scenes and two new scenes) for testing ($37$ sequences). On the EgoBody dataset, we used $82$ sequences for training and $43$ sequences for testing following the default training and test sets provided in the original paper [15].

*b) Evaluation Metric:* As is commonly used in gaze prediction [1], [11], we employed the mean angular error between the generated and ground truth gaze directions (see Equation 5) as the metric to evaluate model performance.

*c) Baselines:* We compared our method with the following state-of-the-art gaze prediction methods that generate eye gaze from human head movements:

- *Head Direction*: *Head Direction* has been frequently used as a proxy for eye gaze due to the strong link between eye and head movements [9], [11], [37].
- *DGaze* [11]: *DGaze* predicts eye gaze from the sequence of head movements using a 1D convolutional neural network.
- *FixationNet* [1]: *FixationNet* extracts features from head movement sequence using a 1D convolutional neural network and combines the features with prior knowledge of gaze distribution to generate eye gaze directions.

*d) Implementation Details:* We trained the baseline methods from scratch using their default parameters. To train our method, we used the Adam optimiser with an initial learning rate of $0.005$ that we decayed by $0.95$ every epoch. We used a batch size of $32$ to train our method for a total of $50$ epochs. We implemented our method using the PyTorch framework.

*e) Generation Settings:* We set our model to generate $15$ frames (corresponding to $500$ ms) of eye gaze directions $G_{t+1:t+15} = \{g_{t+1}, g_{t+2}, ..., g_{t+15}\}$ following the settings used in prior work [1], [11]. We evaluated our method for

three different generation tasks: Generating target eye gaze from past, present, and future body poses, respectively:

- *Generating Gaze from Past Poses*: We used the body poses and head directions in the past 15 frames $P_{t-14:t} = \{p_{t-14}, p_{t-13}, ..., p_t\}$ and $H_{t-14:t} = \{h_{t-14}, h_{t-13}, ..., h_t\}$ as input to generate the target eye gaze. This setting is equivalent to predicting human eye gaze in the future (gaze forecasting) [1], [11], which is important for a variety of applications including visual attention enhancement [41], dynamic event triggering [2], as well as human-human and human-computer interaction [42], [43].

- *Generating Gaze from Present Poses*: We used the body poses and head directions at the present time $P_{t+1:t+15} = \{p_{t+1}, p_{t+2}, ..., p_{t+15}\}$ and $H_{t+1:t+15} = \{h_{t+1}, h_{t+2}, ..., h_{t+15}\}$ as input to generate the corresponding gaze directions. This setting corresponds to estimating human eye gaze in real time [10], [36], which is key for a number of applications including gaze-contingent rendering [3], gaze-based interaction [44], and gaze-guided redirected walking [6].

- *Generating Gaze from Future Poses*: subsection III-C reveals that in human-object interactions eye gaze has highest correlations with body motions in the near future and this implies that using future body poses may improve the performance of gaze generation. Therefore, we used the body poses in the future 15 frames $P_{t+16:t+30} = \{p_{t+16}, p_{t+17}, ..., p_{t+30}\}$ and the head directions at the present time $H_{t+1:t+15} = \{h_{t+1}, h_{t+2}, ..., h_{t+15}\}$ as input to generate the target eye gaze. We used real-time head directions because there exists little or no time delay between head and eye movements (subsection III-B). This setting can be seen as an offline processing way of generating eye movements and is particularly important for the applications that rely on offline analysis of gaze data such as virtual content design and optimisation [5], [9].

## B. Gaze Generation Results

*a) Generating Gaze from Past Poses:* Table IV-*past* summarises the performances of different methods for generating eye gaze from past body poses on the MoGaze, ADT, GIMO, and EgoBody datasets. We can see that our method outperforms the state-of-the-art methods in terms of both individual actions as well as all the actions in a dataset, achieving an average improvement of 22.0% (13.1° *vs.* 16.8°) on MoGaze, 8.0% (11.5° *vs.* 12.5°) on ADT, 11.1% (18.4° *vs.* 20.7°) on GIMO, and 28.6% (13.2° *vs.* 18.5°) on EgoBody. We further performed a paired Wilcoxon signed-rank test to compare the mean angular error of our method and that of the state-of-the-art methods and validated that the differences between our method and the state of the art are statistically significant ($p < 0.01$) on all the four datasets. In addition, we notice that our method achieves the highest improvement (28.6%) on the EgoBody dataset, demonstrating its effectiveness on the challenging human-human interaction setting. We also find that our method's improvement on the ADT dataset (8.0%) is relatively smaller compared with the improvements on other datasets. This is probably because the body motions in the

activities of ADT are less frequent and less correlated with eye gaze (see subsection III-C), thus degrading the performance of our method. The above results demonstrate that our method has a strong capability of predicting eye gaze from past body poses in both human-object and human-human interaction activities.

*b) Generating Gaze from Present Poses:* Table IV-*present* summarises the mean angular errors of different methods for generating eye gaze from present body poses on the MoGaze, ADT, GIMO, and EgoBody datasets. We can see that in terms of both individual actions and all the actions in a dataset, our method achieves better performances than the state of the art. Specifically, our method achieves an average improvement of 19.2% (10.1° *vs.* 12.5°) on MoGaze, 9.1% (9.0° *vs.* 9.9°) on ADT, 17.3% (16.3° *vs.* 19.7°) on GIMO, and 24.9% (13.0° *vs.* 17.3°) on EgoBody. A paired Wilcoxon signed-rank test was performed to compare the mean angular error of our method with that of the state-of-the-art methods and the results indicated that the differences between our method and the state of the art are statistically significant ($p < 0.01$) on all the four datasets. In addition, we find that our method achieves the highest improvement (24.9%) on the EgoBody dataset, demonstrating its superiority for human-human interaction activities. Figure 5 illustrates the prediction results of different methods on the MoGaze and GIMO datasets. We can see that the eye gaze directions predicted by our method are more close to the ground truth compared with that generated by other methods (see supplementary video for more results). These results demonstrate that our method is able to generate eye gaze from present body poses in various daily activities.
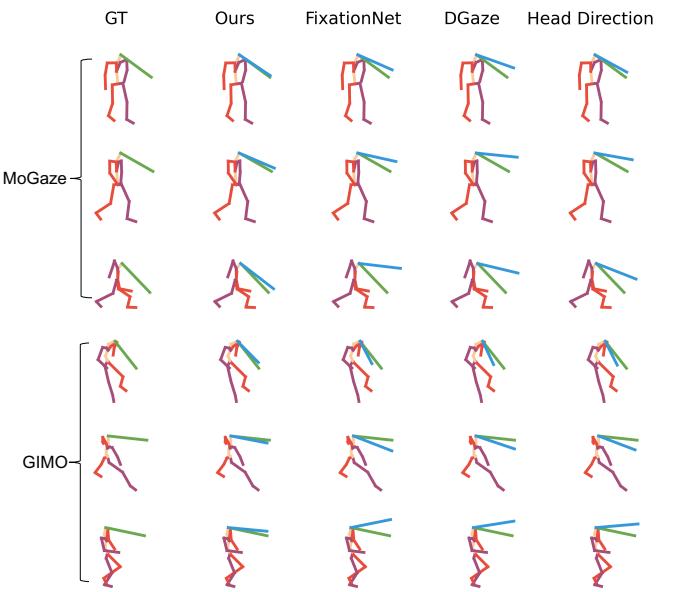


Fig. 5. Results of different methods for generating eye gaze from present poses on the MoGaze and GIMO datasets. The green line indicates the ground truth while the blue line represents the predicted eye gaze.

*c) Generating Gaze from Future Poses:* Table IV-*future* summarises the mean angular errors of different methods for generating eye gaze from future body poses on the MoGaze,

TABLE IV
MEAN ANGULAR ERRORS OF DIFFERENT METHODS FOR GENERATING EYE GAZE FROM PAST, PRESENT, AND FUTURE BODY POSES ON THE MOGAZE, ADT, GIMO, AND EGOBODY DATASETS. BEST RESULTS ARE IN BOLD WHILE THE SECOND BEST ARE UNDERLINED.

| | | MoGaze | | | ADT | | | | GIMO | | | | EgoBody | | | | | | | |
|---|---|---|---|---|---|---|---|---|---|---|---|---|---|---|---|---|---|---|---|---|
| | | pick | place | All | decoration | meal | work | All | change | interact | rest | All | catch | chat | dance | discuss | learn | perform | teach | All |
| past | Head Direction | 37.8° | 34.9° | 36.4° | 26.5° | 30.6° | 27.1° | 28.0° | 23.5° | 23.7° | 22.9° | 23.4° | 14.6° | 18.1° | 25.0° | 18.0° | 17.6° | 16.8° | 24.5° | 19.2° |
| | DGaze [11] | 18.3° | 15.3° | 16.9° | 13.6° | 13.2° | 11.1° | 12.5° | 23.1° | 20.4° | 18.9° | 20.9° | 17.1° | 17.9° | 27.1° | 19.6° | 17.3° | 21.0° | 24.6° | 19.5° |
| | FixationNet [1] | 18.2° | 15.2° | 16.8° | 14.8° | 14.3° | 12.0° | 13.5° | 22.2° | 20.0° | 19.7° | 20.7° | 15.4° | 17.3° | 23.7° | 17.6° | 16.4° | 18.9° | 24.5° | 18.5° |
| | Ours | 15.0° | 11.1° | 13.1° | 12.6° | 12.2° | 10.2° | 11.5° | 17.9° | 21.2° | 16.1° | 18.4° | 12.9° | 13.3° | 19.5° | 16.0° | 8.6° | 13.9° | 13.5° | 13.2° |
| present | Head Direction | 17.6° | 16.2° | 16.9° | 18.5° | 25.3° | 22.9° | 22.3° | 20.9° | 19.9° | 18.6° | 19.8° | 12.4° | 16.8° | 19.0° | 16.6° | 16.6° | 14.3° | 23.7° | 17.7° |
| | DGaze [11] | 13.4° | 12.1° | 12.8° | 10.3° | 10.8° | 8.8° | 9.9° | 22.6° | 20.5° | 17.3° | 20.2° | 14.1° | 16.5° | 22.0° | 16.3° | 15.1° | 17.2° | 24.1° | 17.5° |
| | FixationNet [1] | 13.2° | 11.7° | 12.5° | 11.2° | 11.7° | 9.5° | 10.6° | 21.7° | 19.6° | 17.5° | 19.7° | 13.9° | 16.3° | 21.8° | 16.1° | 15.1° | 17.2° | 23.7° | 17.3° |
| | Ours | 10.7° | 9.4° | 10.1° | 9.5° | 9.8° | 8.1° | 9.0° | 15.9° | 17.3° | 15.9° | 16.3° | 12.1° | 13.5° | 16.7° | 14.2° | 9.7° | 12.0° | 13.0° | 13.0° |
| future | Head Direction | 17.6° | 16.2° | 16.9° | 18.5° | 25.3° | 22.9° | 22.3° | 20.9° | 19.9° | 18.6° | 19.8° | 12.4° | 16.8° | 19.0° | 16.6° | 16.6° | 14.3° | 23.7° | 17.7° |
| | DGaze [11] | 13.4° | 12.1° | 12.8° | 10.3° | 10.8° | 8.8° | 9.9° | 22.6° | 20.5° | 17.3° | 20.2° | 14.1° | 16.5° | 22.0° | 16.3° | 14.8° | 17.2° | 24.1° | 17.5° |
| | FixationNet [1] | 13.2° | 11.7° | 12.5° | 11.2° | 11.7° | 9.5° | 10.6° | 21.7° | 19.6° | 17.5° | 19.7° | 13.9° | 16.3° | 21.8° | 16.1° | 15.1° | 17.2° | 23.7° | 17.3° |
| | Ours | 10.1° | 8.8° | 9.5° | 9.7° | 9.3° | 7.9° | 8.9° | 15.4° | 16.2° | 14.8° | 15.5° | 11.1° | 13.2° | 15.8° | 14.5° | 9.2° | 11.9° | 13.9° | 12.9° |

ADT, GIMO, and EgoBody datasets. We can see that our method outperforms prior methods in both individual actions and all the actions in a dataset, achieving an average improvement of 24.0% (9.5° *vs.* 12.5°) on MoGaze, 10.1% (8.9° *vs.* 9.9°) on ADT, 21.3% (15.5° *vs.* 19.7°) on GIMO, and 25.4% (12.9° *vs.* 17.3°) on EgoBody. A paired Wilcoxon signed-rank test was conducted and the results validated that the differences between our method and the state of the art are statistically significant ($p < 0.01$) in all the four datasets. The above results demonstrate that our method has high performance in generating eye gaze from future body poses in both human-object and human-human interaction activities.

*d) Summary:* The above results demonstrate that our method significantly outperforms the state-of-the-art methods for three different eye gaze generation tasks. Furthermore, we find that in human-object interaction activities, our method achieves significantly higher accuracies using future body poses than using past body poses: 9.5° *vs.* 13.1° on MoGaze, 8.9° *vs.* 11.5° on ADT, and 15.5° *vs.* 18.4° on GIMO. These results correspond with our analysis in subsection III-C that eye gaze has highest correlations with body motions in the near future and suggest that in offline applications where future pose is available, e.g. virtual content design and optimisation [5], [9], using future body poses could generate more accurate eye gaze directions. In human-human interaction activities, we find that our method using past, present, or future body poses achieve similar performances: 13.2° *vs.* 13.0° *vs.* 12.9° on EgoBody. This is because the eye-body correlations in human-human interactions are very close at $-500\ ms$ (past), $0\ ms$ (present) or $500\ ms$ (future), as illustrated in Figure 3b.

*e) Model Size and Time Costs:* Our model has smaller size than the state-of-the-art methods, containing only $0.17M$ trainable parameters while *DGaze* has $0.27M$ parameters and *FixationNet* contains $0.37M$ parameters. We implemented our model on an NVIDIA Tesla V100 SXM2 32GB GPU with an Intel(R) Xeon(R) Platinum 8260 CPU @ 2.40GHz and calculated its time costs. We find that our model requires only 35 ms to train per batch and 3 ms to test per batch, suggesting that our model is fast enough for practical usage.

### C. Ablation Study

We finally performed an ablation study to evaluate the effectiveness of each component used in our model. Specif-

TABLE V
MEAN ANGULAR ERRORS OF DIFFERENT ABLATED VERSIONS OF OUR METHOD ON THE ADT, GIMO, AND EGOBODY DATASETS. *Pose* REFERS TO THE BODY POSE OF THE PERSON WHILE *Pose_I* MEANS THE BODY POSE OF THE INTERACTION PARTNER.

| | | Ours | w/o DCT | w/o S-GCN | w/o T-GCN | w/o Pose | w/o Pose_I | w/o Head |
|---|---|---|---|---|---|---|---|---|
| ADT | past | 11.5° | 11.7° | 11.8° | 11.9° | 12.2° | - | 18.2° |
| | present | 9.0° | 9.1° | 9.4° | 9.1° | 9.5° | - | 17.7° |
| | future | 8.9° | 9.1° | 9.3° | 9.1° | 9.3° | - | 16.4° |
| GIMO | past | 18.4° | 19.0° | 19.3° | 19.1° | 21.2° | - | 22.1° |
| | present | 16.3° | 17.3° | 18.1° | 17.3° | 20.8° | - | 20.9° |
| | future | 15.5° | 16.6° | 18.1° | 16.7° | 20.8° | - | 18.8° |
| EgoBody | past | 13.2° | 13.5° | 13.4° | 13.4° | 20.6° | 18.6° | 15.1° |
| | present | 13.0° | 13.1° | 14.3° | 13.3° | 18.1° | 17.9° | 14.5° |
| | future | 12.9° | 13.7° | 14.8° | 13.5° | 17.1° | 17.9° | 15.1° |

ically, we respectively evaluated different ablated versions of our model that did not contain the *DCT*, *spatial GCN*, *temporal GCN*, the body poses of the person, the body poses of the interaction partner, and the head directions under three generation settings. Table V summarises the mean angular errors of different ablated versions of our method on the ADT, GIMO, and EgoBody datasets. We can see that our method consistently outperforms the ablated methods under different generation settings and the results are statistically significant (paired Wilcoxon signed-rank test, $p < 0.01$), thus underlining the effectiveness of our model architecture. In addition, we find that in human-human interactions removing the body poses of the person or the body poses of the interaction partner significantly degrades the performance of our model: EgoBody-*past* from 13.2° to 20.6° or 18.6°, EgoBody-*present* from 13.0° to 18.1° or 17.9°, EgoBody-*future* from 12.9° to 17.1° or 17.9°. These results demonstrate the effectiveness of the two body poses on generating eye gaze in human-human interaction activities.

## VI. EYE-BASED ACTIVITY RECOGNITION

Activity recognition is a popular task in the area of human-centred computing and has great relevance for many VR/AR scenarios including adaptive virtual environment design [2], low-latency predictive interfaces [45], [46], or human-aware intelligent systems [47]. It is well-known that user activities can be recognised directly from human eye gaze [7], [48]. As such, eye-based activity recognition serves as a particularly relevant sample downstream task to further evaluate our gaze prediction method. The higher the activity recognition accuracy, the better the quality of the predicted gaze sequences.

TABLE VI
EYE-BASED ACTIVITY RECOGNITION ACCURACIES OF USING GROUND
TRUTH EYE GAZE AND THE EYE GAZE PREDICTED FROM DIFFERENT
METHODS ON ADT AND EGOBODY. BEST RESULTS ARE IN BOLD WHILE
THE SECOND BEST ARE UNDERLINED.

|  | GT | Ours | *DGaze* [11] | *FixationNet* [1] | *Head Direction* | *Chance* |
|---|---|---|---|---|---|---|
| ADT | **74.7%** | 70.0% | 67.3% | 66.8% | 40.9% | 33.3% |
| EgoBody | **62.1%** | 60.1% | 52.3% | 58.2% | 50.3% | 33.3% |

*a) Datasets:* We only evaluated on the ADT and Ego-Body datasets given that they provide activity labels for each recorded sequence and their sequence lengths are sufficient ($> 10$ s) for training activity recognition methods [7], [49]. For both datasets, we used the same training and test sets as in section V.

*b) Activity Recognition Method:* We used the state-of-the-art method *EHTask* [7] for activity recognition in VR. *EHTask* takes a sequence of eye gaze data as input, extracts eye features using a 1D CNN and a bidirectional gated recurrent unit (GRU), and finally recognises user activities from the eye features using fully-connected layers.

*c) Procedure:* We first trained *EHTask* to recognise user activities from the ground truth eye gaze sequences using default parameters. On the ADT dataset, we trained *EHTask* to recognise three activities: *decoration*, *meal*, and *work*. On the EgoBody dataset, we trained *EHTask* for three activities that have the most recordings, i.e. *chat*, *learn*, and *teach*. Since activity recognition usually requires a long sequence as input [7], [49], we used 300 frames (corresponding to 10 seconds) of ground truth eye gaze data to train *EHTask* as in the original paper [7]. At test time, we used the eye gaze sequences generated from different methods as input to *EHTask* and evaluated its activity recognition performance. Since the gaze prediction methods were trained to predict 15 frames of eye gaze while *EHTask* requires an input of 300 frames, we first segmented the 300 frames of test data into 20 windows (each window contains 15 frames), then predicted eye gaze for each window, and finally concatenated the gaze predictions of all the windows and used them as input to *EHTask* to recognise user activities.

*d) Results:* Table VI shows the recognition performances of using the ground truth eye gaze and the eye gaze predicted from different methods on ADT and EgoBody. It can be seen in the table that our method achieves higher recognition accuracies than other methods on both ADT (70.0% vs. 67.3%) and EgoBody (60.1% vs. 58.2%). Using a paired Wilcoxon signed-rank test we confirmed that these differences were statistically significant ($p < 0.01$). We also notice that our method can achieve comparable performance with the ground truth eye gaze in terms of recognition accuracy (70.0% vs. 74.7% on ADT, and 60.1% vs. 62.1% on EgoBody). These results illustrate the benefit of our method when using the predicted gaze sequences for downstream tasks with high relevance for VR/AR applications, such as eye-based activity recognition.

## VII. DISCUSSION

In this work we have made an important step towards understanding the correlation between eye and full-body movements in daily activities and generating eye gaze from full-body poses.

*a) Eye-body Coordination:* Our analyses on eye-body coordination in daily activities revealed novel insights for understanding human eye and body movements that we also used to guide the design of our eye-body coordination model. Specifically, in the analysis of correlation between eye gaze and head directions, we found that there exists little or no time delay between head and eye movements (see Figure 1). Therefore, in the task of generating gaze from future poses (see subsection V-A), we used head directions at the present time to generate target eye gaze rather than using future head directions. In the analysis of correlation between eye gaze and body motions, we found that eye gaze is strongly correlated with full-body motions in human-object interactions (see subsection III-C) and has high correlations with the directions between two bodies in human-human interactions (see subsection III-D). Therefore, our model uses features from the body pose of the person to generate eye gaze in human-object interactions and employed the features from the body poses of the person and the interaction partner to predict eye gaze in human-human interactions (see Figure 4). We also found that eye movements precede body motions in human-object interactions (see subsection III-C). Exploiting this, we used future body poses as input to improve the performance of eye gaze generation in situations where future pose information is available (see subsection V-B). The superior performance of our model shows that our analyses are effective and are valuable for the design of future eye-body coordination models.

*b) Pose-based Gaze Prediction:* Prior methods have typically generated eye gaze from head movements while we predict eye gaze from both head movements and full-body poses. This approach proved highly effective and significantly outperforms prior methods in both human-object and human-human interaction activities for three different eye gaze generation tasks (see Table IV). An ablation study confirmed that body poses are instrumental for achieving these performance improvements (see Table V). Taken together, these results underline the significant potential of human full-body poses for generating eye movements and thus open the promising research direction of pose-based gaze prediction.

*c) Applications of Our Method:* In addition to the sample downstream task of eye-based activity recognition (see section VI), we believe that our method has significant potential for numerous VR/AR applications, including dynamic event triggering [2], gaze-contingent rendering [10], [11], gaze-based interaction [24], or virtual content design and optimisation [5], [9]. In addition, with further advances in the development of motion capture and motion generation techniques [16], [19], it will become increasingly easy to obtain human full-body poses in VR and AR environments. In the future, our approach could be integrated with such motion capture and motion generation techniques to generate eye and full-body movements simultaneously.

*d) Limitations and Future Work:* Despite these advances, our work has several limitations that we plan to address in the future. First, we focused on eye-body coordination in

different activities and ignored the influence of the visual scene in front of the person. It will be interesting to explore whether eye-body coordination during the same activity will be affected by different scene content. If so, this will also open a new avenue for research on ways to incorporate visual scene information into the prediction and to see whether this can improve performance further. Second, incorporating other modalities such as facial expressions and audio signals in social interactions may also boost our model's gaze prediction performance. In addition, existing datasets that include body pose and eye gaze have all been collected in indoor environments, thus unfortunately limiting our analyses to indoor settings. It remains to be seen whether eye-body coordination as characterised here also generalises to outdoor scenarios. Furthermore, existing datasets only offer data for interactions between two humans, thus limiting our analyses to dyadic settings. It will be interesting to explore the eye-body coordination during other interaction settings that are important for VR/AR applications, e.g. interactions between more humans and interactions between a human and a virtual avatar. Finally, generating stylistic eye gaze, e.g. eye gaze that can convey different emotions [32], is an interesting avenue for extending our work in the future.

## VIII. CONCLUSION

In this work we were the first to explore the challenging task of predicting human eye gaze from full-body poses. We first conducted a comprehensive analysis on the coordination of human eye and full-body movements in everyday activities and revealed that in human-object interactions eye gaze is strongly correlated with full-body motions while in human-human interactions a person's gaze direction has strong correlations with the directions pointing from his body to the body of the interaction partner. Based on these insights, we proposed a novel eye-body coordination model to predict eye gaze from head directions and full-body poses that outperformed the state-of-the-art methods by a large margin for three different prediction tasks as well as the application of eye-based activity recognition. Taken together, our work provides novel insights into eye-body coordination during daily activities and makes an important step towards pose-based gaze prediction.

## REFERENCES

[1] Z. Hu, A. Bulling, S. Li, and G. Wang, "Fixationnet: forecasting eye fixations in task-oriented virtual environments," *IEEE Transactions on Visualization and Computer Graphics*, vol. 27, no. 5, pp. 2681–2690, 2021.

[2] J. Hadnett-Hunter, G. Nicolaou, E. O'Neill, and M. Proulx, "The effect of task on visual attention in interactive virtual environments," *ACM Transactions on Applied Perception*, vol. 16, no. 3, pp. 1–17, 2019.

[3] A. Patney, M. Salvi, J. Kim, A. Kaplanyan, C. Wyman, N. Benty, D. Luebke, and A. Lefohn, "Towards foveated rendering for gaze-tracked virtual reality," *ACM Transactions on Graphics*, vol. 35, no. 6, pp. 1–12, 2016.

[4] L. Sidenmark and H. Gellersen, "Eye&head: Synergetic eye and head movement for gaze pointing and selection," in *Proceedings of the 2019 Annual ACM Symposium on User Interface Software and Technology*, 2019, pp. 1161–1174.

[5] R. Alghofaili, M. S. Solah, H. Huang, Y. Sawahata, M. Pomplun, and L.-F. Yu, "Optimizing visual element placement via visual attention analysis," in *Proceedings of the 2019 IEEE Conference on Virtual Reality and 3D User Interfaces*. IEEE, 2019, pp. 464–473.

[6] Q. Sun, A. Patney, L.-Y. Wei, O. Shapira, J. Lu, P. Asente, S. Zhu, M. McGuire, D. Luebke, and A. Kaufman, "Towards virtual reality infinite walking: dynamic saccadic redirection," *ACM Transactions on Graphics*, vol. 37, no. 4, pp. 1–13, 2018.

[7] Z. Hu, A. Bulling, S. Li, and G. Wang, "Ehtask: recognizing user tasks from eye and head movements in immersive virtual reality," *IEEE Transactions on Visualization and Computer Graphics*, 2022.

[8] R. Cañigueral and A. F. d. C. Hamilton, "Being watched: Effects of an audience on eye gaze and prosocial behaviour," *Acta Psychologica*, vol. 195, pp. 50–63, 2019.

[9] V. Sitzmann, A. Serrano, A. Pavel, M. Agrawala, D. Gutierrez, B. Masia, and G. Wetzstein, "Saliency in vr: how do people explore virtual environments?" *IEEE Transactions on Visualization and Computer Graphics*, vol. 24, no. 4, pp. 1633–1642, 2018.

[10] Z. Hu, C. Zhang, S. Li, G. Wang, and D. Manocha, "Sgaze: a data-driven eye-head coordination model for realtime gaze prediction," *IEEE Transactions on Visualization and Computer Graphics*, vol. 25, no. 5, pp. 2002–2010, 2019.

[11] Z. Hu, S. Li, C. Zhang, K. Yi, G. Wang, and D. Manocha, "Dgaze: Cnn-based gaze prediction in dynamic scenes," *IEEE Transactions on Visualization and Computer Graphics*, vol. 26, no. 5, pp. 1902–1911, 2020.

[12] P. Kratzer, S. Bihlmaier, N. B. Midlagajni, R. Prakash, M. Toussaint, and J. Mainprice, "Mogaze: A dataset of full-body motions that includes workspace geometry and eye-gaze," *IEEE Robotics and Automation Letters*, vol. 6, no. 2, pp. 367–373, 2020.

[13] X. Pan, N. Charron, Y. Yang, S. Peters, T. Whelan, C. Kong, O. Parkhi, R. Newcombe, and Y. C. Ren, "Aria digital twin: A new benchmark dataset for egocentric 3d machine perception," in *Proceedings of the IEEE/CVF International Conference on Computer Vision*, 2023, pp. 20 133–20 143.

[14] Y. Zheng, Y. Yang, K. Mo, J. Li, T. Yu, Y. Liu, K. Liu, and L. J. Guibas, "Gimo: Gaze-informed human motion prediction in context," in *Proceedings of the 2022 European Conference on Computer Vision*, 2022.

[15] S. Zhang, Q. Ma, Y. Zhang, Z. Qian, M. Pollefeys, F. Bogo, and S. Tang, "Egobody: Human body shape, motion and social interactions from head-mounted devices," in *Proceedings of the 2022 European Conference on Computer Vision*, 2022.

[16] D. Hasegawa, N. Kaneko, S. Shirakawa, H. Sakuta, and K. Sumi, "Evaluation of speech-to-gesture generation using bi-directional lstm network," in *Proceedings of the 2018 International Conference on Intelligent Virtual Agents*, 2018, pp. 79–86.

[17] T. Kucherenko, D. Hasegawa, G. E. Henter, N. Kaneko, and H. Kjellström, "Analyzing input and output representations for speech-driven gesture generation," in *Proceedings of the 2019 ACM International Conference on Intelligent Virtual Agents*, 2019, pp. 97–104.

[18] Y. Yoon, W.-R. Ko, M. Jang, J. Lee, J. Kim, and G. Lee, "Robots learn social skills: End-to-end learning of co-speech gesture generation for humanoid robots," in *Proceedings of the 2019 International Conference on Robotics and Automation*. IEEE, 2019, pp. 4303–4309.

[19] U. Bhattacharya, N. Rewkowski, A. Banerjee, P. Guhan, A. Bera, and D. Manocha, "Text2gestures: A transformer-based network for generating emotive body gestures for virtual agents," in *Proceedings of the 2021 IEEE Virtual Reality and 3D User Interfaces*. IEEE, 2021, pp. 1–10.

[20] Z. Ye, H. Wu, J. Jia, Y. Bu, W. Chen, F. Meng, and Y. Wang, "Choreonet: Towards music to dance synthesis with choreographic action unit," in *Proceedings of the 2020 ACM International Conference on Multimedia*, 2020, pp. 744–752.

[21] H.-Y. Lee, X. Yang, M.-Y. Liu, T.-C. Wang, Y.-D. Lu, M.-H. Yang, and J. Kautz, "Dancing to music," *Advances in Neural Information Processing Systems*, vol. 32, 2019.

[22] K. Higuch, R. Yonetani, and Y. Sato, "Can eye help you? effects of visualizing eye fixations on remote collaboration scenarios for physical

tasks," in *Proceedings of the 2016 CHI Conference on Human Factors in Computing Systems*, 2016, pp. 5180–5190.

[23] N. F. Duarte, M. Raković, J. Tasevski, M. I. Coco, A. Billard, and J. Santos-Victor, "Action anticipation: Reading the intentions of humans and robots," *IEEE Robotics and Automation Letters*, vol. 3, no. 4, pp. 4132–4139, 2018.

[24] A. T. Duchowski, "Gaze-based interaction: a 30 year retrospective," *Computers and Graphics*, vol. 73, pp. 59–69, 2018.

[25] C. Jiao, Z. Hu, M. Bâce, and A. Bulling, "Supreyes: Super resolution for eyes using implicit neural representation learning," in *Proceedings of the 2023 Annual ACM Symposium on User Interface Software and Technology*, 2023, pp. 1–13.

[26] J. S. Stahl, "Amplitude of human head movements associated with horizontal saccades," *Experimental Brain Research*, vol. 126, no. 1, pp. 41–54, 1999.

[27] Y. Fang, R. Nakashima, K. Matsumiya, I. Kuriki, and S. Shioiri, "Eye-head coordination for visual cognitive processing," *PloS One*, vol. 10, no. 3, p. e0121035, 2015.

[28] R. Kothari, Z. Yang, C. Kanan, R. Bailey, J. B. Pelz, and G. J. Diaz, "Gaze-in-wild: a dataset for studying eye and head coordination in everyday activities," *Scientific Reports*, vol. 10, no. 1, pp. 1–18, 2020.

[29] L. Sidenmark and H. Gellersen, "Eye, head and torso coordination during gaze shifts in virtual reality," *ACM Transactions on Computer-Human Interaction*, vol. 27, no. 1, pp. 1–40, 2019.

[30] A. U. Batmaz, A. K. Mutasim, M. Malekmakan, E. Sadr, and W. Stuerzlinger, "Touch the wall: Comparison of virtual and augmented reality with conventional 2d screen eye-hand coordination training systems," in *Proceedings of the 2020 IEEE Conference on Virtual Reality and 3D User Interfaces*. IEEE, 2020, pp. 184–193.

[31] K. J. Emery, M. Zannoli, J. Warren, L. Xiao, and S. S. Talathi, "Openneeds: A dataset of gaze, head, hand, and scene signals during exploration in open-ended vr environments," in *Proceedings of the 2021 ACM Symposium on Eye Tracking Research and Applications*, 2021, pp. 1–7.

[32] T. Randhavane, A. Bera, K. Kapsaskis, R. Sheth, K. Gray, and D. Manocha, "Eva: Generating emotional behavior of virtual agents using expressive features of gait and gaze," in *Proceedings of the 2019 ACM Symposium on Applied Perception*, 2019, pp. 1–10.

[33] L. Itti, C. Koch, and E. Niebur, "A model of saliency-based visual attention for rapid scene analysis," *IEEE Transactions on Pattern Analysis and Machine Intelligence*, vol. 20, no. 11, pp. 1254–1259, 1998.

[34] M.-M. Cheng, N. J. Mitra, X. Huang, P. H. Torr, and S.-M. Hu, "Global contrast based salient region detection," *IEEE Transactions on Pattern Analysis and Machine Intelligence*, vol. 37, no. 3, pp. 569–582, 2015.

[35] A. Borji, D. N. Sihite, and L. Itti, "Probabilistic learning of task-specific visual attention," in *Proceedings of the 2012 IEEE Conference on Computer Vision and Pattern Recognition*. IEEE, 2012, pp. 470–477.

[36] G. A. Koulieris, G. Drettakis, D. Cunningham, and K. Mania, "Gaze prediction using machine learning for dynamic stereo manipulation in games," in *Proceedings of the 2016 IEEE Virtual Reality*. IEEE, 2016, pp. 113–120.

[37] R. Nakashima, Y. Fang, Y. Hatori, A. Hiratani, K. Matsumiya, I. Kuriki, and S. Shioiri, "Saliency-based gaze prediction based on head direction," *Vision Research*, vol. 117, pp. 59–66, 2015.

[38] Z. Hu, "Eye fixation forecasting in task-oriented virtual reality," in *Proceedings of the 2021 IEEE Conference on Virtual Reality and 3D User Interfaces Abstracts and Workshops*. IEEE, 2021, pp. 707–708.

[39] T. Ma, Y. Nie, C. Long, Q. Zhang, and G. Li, "Progressively generating better initial guesses towards next stages for high-quality human motion prediction," in *Proceedings of the 2022 IEEE Conference on Computer Vision and Pattern Recognition*, 2022, pp. 6437–6446.

[40] W. Mao, M. Liu, and M. Salzmann, "History repeats itself: Human motion prediction via motion attention," in *Proceedings of the 2020 European Conference on Computer Vision*. Springer, 2020, pp. 474–489.

[41] M. S. El-Nasr, A. Vasilakos, C. Rao, and J. Zupko, "Dynamic intelligent lighting for directing visual attention in interactive 3d scenes," *IEEE Transactions on Computational Intelligence and AI in Games*, vol. 1, no. 2, pp. 145–153, 2009.

[42] J. Steil, P. Müller, Y. Sugano, and A. Bulling, "Forecasting user attention during everyday mobile interactions using device-integrated and wearable sensors," in *Proceedings of the 2018 ACM International Conference on Human-Computer Interaction with Mobile Devices and Services*, 2018, pp. 1:1–1:13.

[43] P. Müller, E. Sood, and A. Bulling, "Anticipating averted gaze in dyadic interactions," in *Proceedings of the 2020 ACM International Symposium on Eye Tracking Research and Applications*, 2020, pp. 1–10.

[44] P. Majaranta and A. Bulling, *Eye Tracking and Eye-Based Human-Computer Interaction*. Springer Publishing London, 2014, pp. 39–65.

[45] B. David-John, C. E. Peacock, T. Zhang, T. S. Murdison, H. Benko, and T. R. Jonker, "Towards gaze-based prediction of the intent to interact in virtual reality," in *Proceedings of the 2021 ACM Symposium on Eye Tracking Research and Applications*, 2021, pp. 1–7.

[46] A. Keshava, A. Aumeistere, K. Izdebski, and P. Konig, "Decoding task from oculomotor behavior in virtual reality," in *Proceedings of the 2020 ACM Symposium on Eye Tracking Research and Applications*, 2020, pp. 1–5.

[47] L.-M. Vortmann and F. Putze, "Attention-aware brain computer interface to avoid distractions in augmented reality," in *Extended Abstracts of the 2020 CHI Conference on Human Factors in Computing Systems*, 2020, pp. 1–8.

[48] A. Bulling, J. A. Ward, H. Gellersen, and G. Troster, "Eye movement analysis for activity recognition using electrooculography," *IEEE Transactions on Pattern Analysis and Machine Intelligence*, vol. 33, no. 4, pp. 741–753, 2010.

[49] A. Coutrot, J. H. Hsiao, and A. B. Chan, "Scanpath modeling and classification with hidden markov models," *Behavior Research Methods*, vol. 50, no. 1, pp. 362–379, 2018.

## IX. BIOGRAPHY SECTION



**Zhiming Hu** is a post-doctoral researcher at the University of Stuttgart, Germany. He obtained his Ph.D. degree in Computer Software and Theory from Peking University, China in 2022 and received his Bachelor's degree in Optical Engineering from Beijing Institute of Technology, China in 2017. His research interests include virtual reality, human-computer interaction, eye tracking, and human-centred artificial intelligence.



**Jiahui Xu** is a master student at the University of Stuttgart, Germany. She received her Bachelor's degree in Electronic Information Engineering from Jilin University, China in 2019. Her research interests include human-computer interaction, computer vision, and virtual reality.



**Syn Schmitt** is Full Professor of Biomechanics and Biorobotics at the University of Stuttgart, Germany, where he directs the research group "Computational Biophysics and Biorobotics". He received his MSc. in Physics from the University of Stuttgart, Germany, in 2003 and his PhD in Theoretical Physics from University of Tübingen, Germany, in 2006. His research interests include biomechanics, neuromechanics, biorobotics.



**Andreas Bulling** is Full Professor of Computer Science at the University of Stuttgart, Germany, where he directs the research group "Human-Computer Interaction and Cognitive Systems". He received his MSc. in Computer Science from the Karlsruhe Institute of Technology, Germany, in 2006 and his PhD in Information Technology and Electrical Engineering from ETH Zurich, Switzerland, in 2010. Before, Andreas Bulling was a Feodor Lynen and Marie Curie Research Fellow at the University of Cambridge, UK, and a Senior Researcher at the Max Planck Institute for Informatics, Germany. His research interests include computer vision, machine learning, and human-computer interaction.